

# Photocatalytic performance of Ag-modified natural zeolite catalyst for photocatalysis degradation of Methylene Blue (MB) under VIS irradiation

L. A. Colar<sup>1</sup>, A. Jakab<sup>1</sup>, F. Manea<sup>1</sup>, R. Pode<sup>1</sup> & C. Orha<sup>2</sup>

<sup>1</sup>*Faculty of Industrial Chemistry and Environmental Engineering, "Politehnica" University of Timisoara, Romania*

<sup>2</sup>*Department of Condensed Matter, National Institute of Research-Development for Electrochemistry and Matter, Timisoara, Romania*

## Abstract

In this study, Ag-modified natural zeolite catalyst (Z-Ag<sub>red</sub>) was synthesized by chemical activation prior to the ion exchange and followed by a silver reduction with sodium boron hydride. The surface characterization of Z-Ag<sub>red</sub> has been investigated by X-ray diffraction, FT-IR spectroscopy, SEM microscopy and EDX analysis. Also, UV-VIS diffuse reflectance (DRUV-VIS) spectroscopy was used to determine the light absorption properties of the catalyst. The effect of silver reduction was noticed by comparison with the characterization of silver-modified natural zeolite by ion-exchange without the reduction stage. The photocatalytic performance of Z-Ag<sub>red</sub> catalyst was proved by photocatalysis application for the decolorisation and degradation of Methylene Blue (MB) dye containing wastewater under visible irradiation. The optimum operating parameters were determined based on the assessment of the photocatalytic process efficiency as a function of the catalyst dose, the initial pH, and the initial concentration of dye. The good results regarding the photocatalytic degradation of MB dye using Z-Ag<sub>red</sub> catalyst claim it as a potential for the real photocatalysis application in MB-containing wastewater under solar light.

*Keywords: Ag-modified natural zeolite catalyst, photocatalysis, VIS irradiation, MB dye.*



## 1 Introduction

Dyes are widely used as coloring agents in a variety of industries, such as textiles, cosmetics, pulp mills, printing, foods, and plastics. Because many organic dyestuffs are harmful to human beings and hazardous to aquatic organisms, removal of dyestuffs from wastewater has received considerable attention over the past decades.

In order to handle the dye removal from water, various methods have been investigated. Among biodegradation, methods like coagulation [1], adsorption [2] and advanced oxidation processes (AOPs) [3, 4] have been employed. All these processes exhibit some specific advantages or drawbacks.

Among AOPs, heterogeneous photocatalysis is considered to be one of the most emerging oxidation technology due to the lack of limitations in mass transfer, the ability to be carried out under ambient conditions (atmospheric oxygen is used as oxidant), and may lead to complete mineralization of organic carbon to  $\text{CO}_2$ .

The incorporation of transition metals with different oxidation states into zeolites has been studied to develop materials with potential applications in many fields, as catalysis and water treatment [5, 6].

The aim of this work was to evaluate the photocatalytic performance of Ag-modified natural zeolite for photocatalysis degradation of Methylene Blue (MB) under VIS irradiation. The catalyst was structurally characterized and the photocatalytic activity was determined for MB dye degradation under VIS irradiation.

## 2 Materials and methods

### 2.1 Chemicals

Methylene Blue (MB) (commercial grade) with a molecular weight of  $373.9 \text{ g}\cdot\text{mol}^{-1}$  was supplied by Pekin Chemical Works Peking (China).

The chemical used for synthesis, *i.e.*, silver nitrate ( $\text{AgNO}_3$ ) hydrochloric acid (HCl), sodium chloride (NaCl), sodium boron hydride ( $\text{NaBH}_4$ ) were purchased from Merck Company. Romanian zeolitic mineral from Mirsid was supplied by CEMACON Company, Romania. The mineral was powdered and sieved with a Multilab sieve shaker. The mass composition of the mineral is: 62.20%, wt.  $\text{SiO}_2$ , 11.65%, wt.  $\text{Al}_2\text{O}_3$ , 1.30%, wt.  $\text{Fe}_2\text{O}_3$ , 3.74%, wt. CaO, 0.67%, wt. MgO, 3.30%, wt.  $\text{K}_2\text{O}$ , 0.72%, wt.  $\text{Na}_2\text{O}$ , 0.28%, wt.  $\text{TiO}_2$ .

### 2.2 Preparation of Ag-modified natural zeolite (Z-Ag<sub>red</sub>) catalyst

Ag-modified natural zeolite (Z-Ag<sub>red</sub>) catalyst was synthesized by a chemical activation prior to the ion exchange and followed by a silver reduction with sodium boron hydride. The preparation of the chemically modified zeolite presumes two stages to reach acid form (H form) by using 1 M HCl solution and sodium form (Na form) with 1 M NaCl solution for a more efficient ion exchange.

For preparation of  $\text{Ag}^+$ -modified zeolite (Z-Ag), Na form of zeolite was added to a volume of 0.03 M  $\text{Ag}^+$  solution (as nitrate salt) corresponding to a solid/liquid ratio of 1/100. The ion exchange process has been conducted under magnetic stirring, at room temperature, for 8 h. The Z-Ag material was filtered off, washed with water and dried at  $100^\circ\text{C}$ . Z- $\text{Ag}_{\text{red}}$  catalyst was obtained by the reduction process of Z-Ag using a 0.04 M  $\text{NaBH}_4$  solution ( $\text{pH}=12$ ), at 1/4 molar ratio of  $\text{Ag}/\text{NaBH}_4$ . The Z- $\text{Ag}_{\text{red}}$  catalyst was separated by centrifugation and subjected to the repeated washing-centrifugation, until disappearance of residual alkalinity.

### 2.3 Characterization of the photocatalyst

The crystallinity of the prepared samples was measured by X-ray diffraction (XRD) using PANalytical X<sup>3</sup>PertPRO MPD Diffractometer with a Cu tube.

The light absorption properties of the materials were studied by UV–VIS diffuse reflectance spectroscopy (DRUV–VIS), performed under ambient conditions using Lambda 950 Perkin Elmer in the wavelength range of 200–600 nm. The bond vibration of the catalyst was analyzed by Fourier transform infrared spectrometry (FT-IR) using a JASCO FT/IR-430 spectrometer. The surface morphology was studied by a scanning electron microscopy coupled with the energy dispersive X-ray analysis (SEM/EDX), using Inspect S PANalytical model detector.

### 2.4 Photocatalytic experiments

All experiments regarding adsorption and photocatalysis processes were carried out under magnetic stirring at  $20^\circ\text{C}$  into a RS-1 photo-catalytic reactor (Heraeus, Germany), which consists of a submerged lamp surrounded by a quartz shield. Solutions of MB dye at different concentrations (prepared from an initial stock solution of  $1\text{g}\cdot\text{L}^{-1}$ ) were placed into the photoreactor and irradiated with an UV light set between 280 and 360 nm when UV photocatalytic process was employed, and with a VIS light set between 460 and 510 nm in the case of VIS photocatalytic process, for 180 minutes. A system of water recirculation maintained a constant temperature of  $20^\circ\text{C}$  for the whole period of photocatalytic experiments.

The catalyst was placed into 400 mL MB solution. Prior to irradiation, the suspension was stirred continuously in the dark for 30 min to reach the steady-state conditions. The concentration of the dye in the bulk solution at the end point of the adsorption step was considered as the initial concentration value for the investigation of the photocatalytic process. At regular time intervals of irradiation, samples were collected and filtered through a Milipore filter (pore size of  $0.45\ \mu\text{m}$ ) in order to remove the zeolite from the aqueous solution. The concentration of MB solutions was measured with a Varian Cary 100 UV-VIS spectrophotometer.

The assessment of the photocatalysis performance was carried out as discoloration and degradation efficiencies. The discoloration and degradation efficiencies were determined based on the absorbance recorded at 663 nm and



291 nm, respectively. The pH of dye solutions was adjusted by adding diluted  $\text{H}_2\text{SO}_4$  and  $\text{NaOH}$  solutions (analytical grade), using an Inolab pH-meter.

### 3 Results and discussion

#### 3.1 Structural and morphological characterization of Z- $\text{Ag}_{\text{red}}$ catalyst

##### 3.1.1 XRD analysis

The XRD pattern of Ag-modified natural zeolite catalyst (Z- $\text{Ag}_{\text{red}}$ ) is illustrated in fig. 1. For comparison, the XRD patterns of the natural zeolite in Na form (fig.1, spectrum (a)) and of the  $\text{Ag}^+$ -modified zeolite (Z- $\text{Ag}$ ) are also shown (fig.1, spectrum (b)).

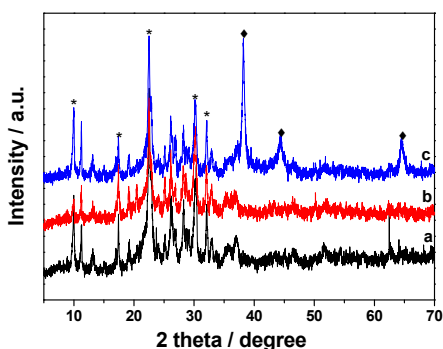


Figure 1: XRD patterns for (a) Z-Na, (b) Z-Ag and (c) Z- $\text{Ag}_{\text{red}}^*$ -clinoptilolite; ♦-metallic silver.

It can be seen that the main peak positions of natural zeolite (clinoptilolite) (2 theta: 9.92°; 22.5°; 25.8°; 30.05°; 32°) [7] are found also in the XRD pattern of the natural zeolite in Na form. The peak corresponding to 2 theta ~ 26.6° is attributed to  $\text{Na}^+$  presence within zeolite lattice.

The study of the XRD patterns confirms that no transition of zeolite phases occurred during  $\text{Ag}^+$  ion exchange. Variations in the relative intensities of the clinoptilolite peaks (2 theta: 9.92°; 11.2°) were found in the XRD pattern of Z-Ag, after Ag ion exchange. These variations can be associated mainly with differences in the nature, amount and position of the extra-framework species in clinoptilolite channels [8]. The presence of new peaks (2 theta: 38.1°; 44.3°; 64.5°) can be attributed to the presence of metallic Ag, which confirmed the occurrence of reduction process of Ag ions [9].

##### 3.1.2 DRUV-VIS spectroscopy

Figure 2 presents the DRUV-VIS spectra of Na form of zeolite (a), Z-Ag after ion exchange process (b) and Ag-modified natural zeolite catalyst (Z- $\text{Ag}_{\text{red}}$ ) after reduction process (c).

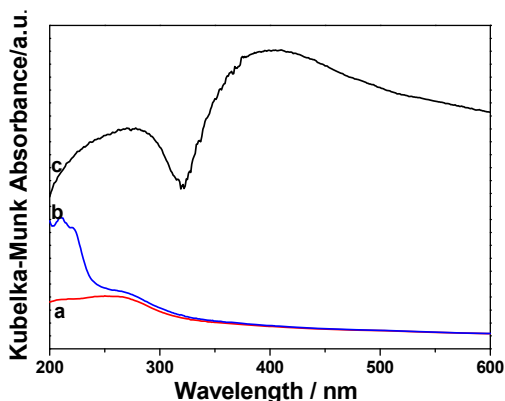


Figure 2: DRUV-VIS spectra of (a) Z-Na, (b) Z-Ag and (c) Z-Ag<sub>red</sub>.

DRUV-VIS patterns are examined to determine the light absorption quantification and absorption wavelength range correlated with band gap energy.

After ion exchange appearance of a new peak at 210 nm, assigned to  $\text{Ag}^+$  ions is observed in the spectra of Z-Ag (fig. 2(b)) [9]. This peak disappeared in the Z-Ag<sub>red</sub> spectrum, which exhibits two broad absorption bands (Fig. 2(c)). The first one, with asymmetric peak centered at 276 nm, is attributed to small  $\text{Ag}_4^{\delta+}$  clusters [8]. The other one, in visible region, with asymmetric peak centered at 400 nm, is assigned to silver particles [9]. The relative intensity of the second band (in visible region) is higher than the relative intensity of the first band, which indicates the higher contribution of silver particles compared with the  $\text{Ag}_4^{\delta+}$  clusters, a desired aspect regarding the photocatalytic process.

### 3.1.3 FT-IR analysis

The structural information about the Na form of clinoptilolite (fig. 3(a)) and Z-Ag<sub>red</sub> photocatalyst (fig. 3(b)) were obtained by FT-IR spectroscopy.

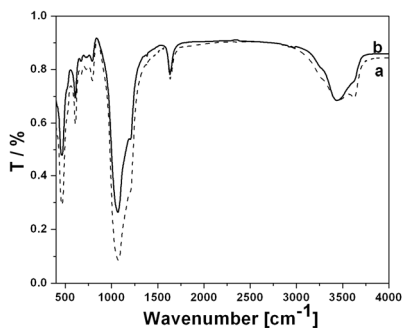


Figure 3: FT-IR spectra of (a) Z-Na and (b) Z-Ag<sub>red</sub>.

Peaks related to the isolated and H-bonded O-H stretching at 3625 and 3450  $\text{cm}^{-1}$ , respectively, were identified in the FT-IR spectra of Z-Na sample (fig.4(a)) [7]. The peak at 3625  $\text{cm}^{-1}$  disappeared in the spectra of Z-Ag<sub>red</sub> sample (Fig. 3(b)), but a shoulder can be observed at the same wave number. In the spectra of Z-Ag<sub>red</sub> sample, the peak centered at 3450  $\text{cm}^{-1}$  characterised by the same intensity but slightly narrowed can be observed.

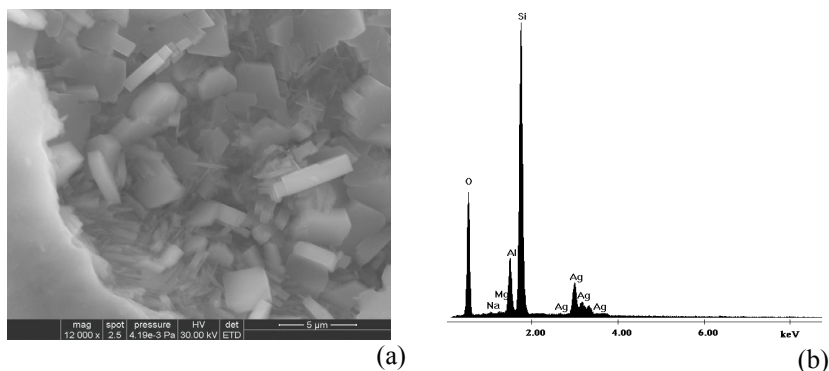


Figure 4: SEM morphology (a) and EDX spectra (b) for Z-Ag<sub>red</sub>.

The peak at 1630 (Lewis sites) is assigned to the zeolitic water in the channels of the samples [10], which is found in the Z-Ag<sub>red</sub> spectrum also. The range between 1250 and 430  $\text{cm}^{-1}$  is composed of four bands centered at 463, 609, 790 and 1070  $\text{cm}^{-1}$ , with a shoulder at 1200  $\text{cm}^{-1}$ , which are characteristic to clinoptilolite and correspond to the symmetric and asymmetric vibration of the (Al, Si) O group [11].

All vibrations bands between 1250 and 430  $\text{cm}^{-1}$  characteristic to clinoptilolite are found in the FT-IR spectrum of Z-Ag<sub>red</sub> sample. FT-IR spectrum of Z-Ag<sub>red</sub> sample is similar as Z-Na, the intensities of the peaks being slight reduced, especial for the external groups. Based on these results, it can be concluded that the reduced silver particles are located onto the zeolite surface [11].

### 3.1.4 Scanning electron microscopy (SEM) and energy dispersive X-ray analysis (EDX) results

The SEM image and EDX spectra of the Z-Ag<sub>red</sub> photocatalyst is presented in fig. 4.

No changes were observed in the morphology of the Z-Ag<sub>red</sub> sample (Fig. 4(a)) in comparison to Na form of zeolite [12].

## 3.2 VIS photocatalytic degradation

The photocatalytic performance of Z-Ag<sub>red</sub> catalyst was studied as a function of pH, catalyst dose and the initial dye concentration under VIS irradiation.

### 3.2.1 pH influence

The influence of pH on the degradation and decolorization of MB dye in aqueous solution was studied in the pH range of 3 to 11 (Fig. 5(a),(b)).

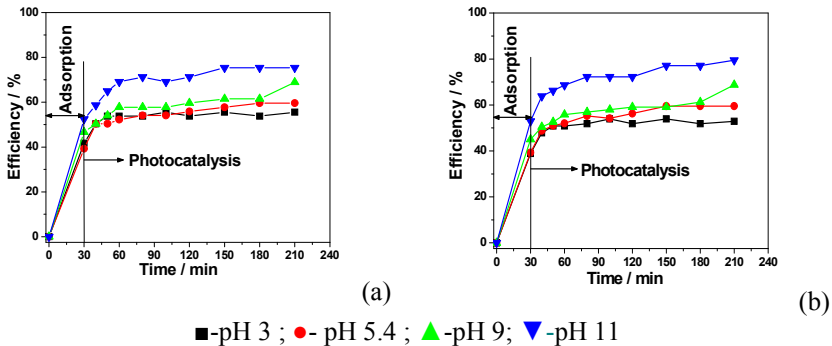


Figure 5: Efficiencies of MB degradation (a) and decolorization (b) at pH 3-11, during VIS irradiation. Conditions:  $50 \text{ mg}\cdot\text{L}^{-1}$  MB dye;  $1 \text{ g}\cdot\text{L}^{-1}$   $\text{Z-Ag}_{\text{red}}$ .

pH changes can influence the adsorption of the dye molecules onto the catalyst surface, an important step for the photocatalytic oxidation. It can be seen that the adsorption degree increased with pH shifting from acidic to alkaline medium, and a maximum degree is reached at pH 11 (~53%). This phenomenon is given by the dye nature and the catalyst surface charge. MB is a cationic dye and the catalyst surface charge shifts to more negative value with pH increasing, and the electrostatic attraction between dye molecule and catalytic surface is favored. Taking into consideration that the heterocatalytic oxidation mechanism involves the electron-hole pair generation, the alkaline medium should favors the photocatalytic oxidation, the aspect proved by its pH dependence. Also, the alkaline medium provides a larger concentration of hidroxil ions available to generate  $\text{HO}^\bullet$  radicals. Because the photocatalysis contribution in the global efficiency was almost the same at both pH values of 9 and 11 (about 23% degradation; 25% decoloration at 180 min irradiation time), the further studies were carried out at pH 9.

### 3.2.2 Effect of catalyst dose

In order to determine the optimum catalyst loading, the degradation of MB dye was investigated using different catalyst concentrations in the range of  $0.25$ - $1.5 \text{ g}\cdot\text{L}^{-1}$ . The results are presented in fig. 6, and it can be observed that increasing the catalyst dose from  $0.25$  to  $1.5 \text{ g}\cdot\text{L}^{-1}$  lead to increasing the dye decoloration efficiency from 22.3 to 83.9%. This may be attributed to the enhanced generation of  $\text{HO}^\bullet$  from the photocatalyst surface based on increasing the photocatalyst amount in the reaction solution. A similar behavior is noticed in the case of degradation efficiency, where the efficiency increases with the catalyst dose increasing up to  $1.5 \text{ g}\cdot\text{L}^{-1}$ .

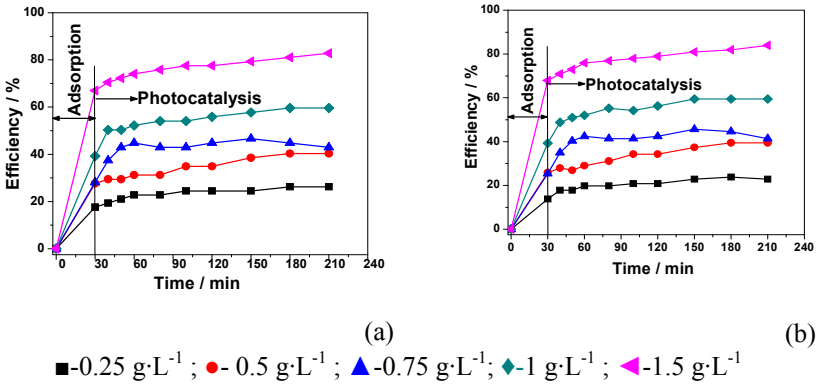


Figure 6: Influence of dose on degradation (a) and discoloration (b) efficiency under VIS irradiation. Conditions: 50 mg·L<sup>-1</sup> MB dye; pH = 5.4.

Based on the process efficiency evolution at the doses of 1.0 and 1.5 g·L<sup>-1</sup>, it can be noticed that even if the adsorption degree is significantly improved at 1.5 g·L<sup>-1</sup> catalyst in comparison with 1.0 g·L<sup>-1</sup>, nevertheless the similar photocatalysis contribution was achieved for both doses, and 1.0 g·L<sup>-1</sup> is selected as optimum dose.

**3.2.3 Effect of the initial dye concentrations**

The photodegradation efficiency depends on the initial dye concentration based on two main aspects.

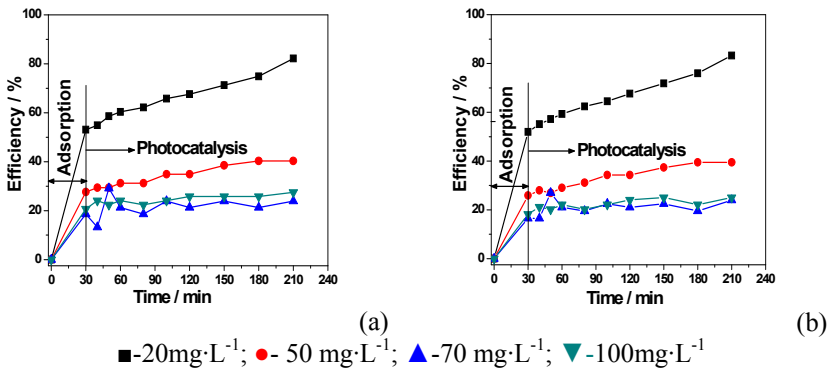


Figure 7: Influence of initial dye concentration on degradation (a) and discoloration (b) efficiency under VIS irradiation. Conditions: 1g·L<sup>-1</sup> Z-Ag<sub>red</sub>; pH = 5.4; reaction temperature-20°C.





The amount of dye adsorbed on the catalytic surface increases with the dye concentration in relation with the available surface, which enhances the catalytic efficiency of the photocatalyst. On the other hand, higher concentration of the dye affects negatively the VIS light penetrability in the dye solution.

The influence of various initial dye concentrations on the photocatalytic discoloration and degradation has been investigated in the concentration range of 25-100 mg·L<sup>-1</sup> MB dye. The results show that the degradation/discoloration process efficiency decreased with initial dye increasing.

## 4 Conclusion

The Z-Ag<sub>red</sub> photocatalyst was successfully synthesized by a chemical activation through ion exchange followed by a silver reduction with sodium boron hydride. The slight variations in the relative intensities of the clinoptilolite peaks found in the XRD pattern of Z-Ag<sub>red</sub> could be associated mainly with differences in the nature, amount and position of the extra-framework species in clinoptilolite channels. The presence of metallic Ag onto zeolite was proved by XRD and also, confirmed by EDX analysis. The DRUV-VIS spectra indicated that Z-Ag<sub>red</sub> exhibited the large absorption bands significantly shifted to the visible range. Silver location into clinoptilolite network, positioned rather at the external zeolite surface was found from FTIR results. The photocatalytic activity of the Z-Ag<sub>red</sub> photocatalyst under VIS irradiation was proved for the degradation of MB dye solution. The solution pH value of 9 and the photocatalyst dose of 1g·L<sup>-1</sup> were established as optimal conditions for photocatalysis application in the degradation of RY 125 dye solution. The photocatalyst exhibited a good performance for discoloration and degradation processes especially at low concentrations, showing a real potential for practical photodegradation application under solar irradiation.

## Acknowledgements

This work was supported by the strategic grant POSDRU 2009 project ID 50783 and ID 77265 of the Ministry of Labour, Family and Social Protection, Romania, co-financed by the European Social Fund – Investing in People, and partially from PN-II-ID-PCE-165/2011.

## References

- [1] Gaoa, B., Liua, B., Chena, T., and Yuea, Q., Effect of aging period on the characteristics and coagulation behavior of polyferric chloride and polyferric chloride–polyamine composite coagulant for synthetic dyeing wastewater treatment. *Journal of Hazardous Materials*, **187(1-3)**, pp. 413–420, 2011.
- [2] Qiu, Qiu, M., Qian, C., Xu, J., Wu, J. and Wang, G., Studies on the adsorption of dyes into clinoptilolite. *Desalination*, **243**, pp. 286–292, 2009.



- [3] El-Desoky, H. S., Ghoneim, M. M., and Zidan, N. M. Decolorization and degradation of Ponceau S azo-dye in aqueous solutions by the electrochemical advanced Fenton oxidation. *Desalination*, **264**, pp. 143–150, 2010.
- [4] Riga, A., Soutsas, K., Ntampeglitis, K., Karayannis and V., Papapolymerou G. G., Effect of system parameters and of inorganic salts on the decolorization and degradation of Procion H-exl dyes. Comparison of H<sub>2</sub>O<sub>2</sub>/UV, UV/Fenton, TiO<sub>2</sub>/UV and TiO<sub>2</sub>/UV/H<sub>2</sub>O<sub>2</sub> processes. *Desalination*, **211**, pp. 72–86, 2007.
- [5] Gurin V.S., Petranovskii V.P., Hernandez M.-A., Bogdanchikova N. and Alexeenko A.A., Silver and copper clusters and small particles, stabilized within nanoporous silicate-based materials. *Materials Science and Engineering*, **A 391**, pp. 71–76, 2005.
- [6] Patterson H.H., Gomez R.S., Lu H. and Yson R.L., Nanoclusters of silver doped in zeolites as photocatalysts. *Catalysis Today* **120**, pp. 168–173, 2007.
- [7] Çağlar Duvarci Ö., Akdeniz Y., Özmiñçi F., Ülkü S., Balköse D. and Çiftçiöğlü M., Thermal behaviour of a zeolitic tuff. *Ceramics International* **33(5)** pp. 795–801, 2007.
- [8] Concepción-Rosabal B., Rodríguez- Fuentes G., Bogdanchikova N., Bosch Bosch P. and Lara V.H., Comparative study on natural and synthetic Clinoptilolites containing silver in different states. *Microporous and Mesoporous Materials*, **86**, pp. 249–255, 2005.
- [9] Bogdanchikova N., Concepción-Rosabal B., Petranovskii V., Avalos-Borja M. and Rodríguez- Fuentes G., Different silver states stabilized in natural clinoptilolite. *Proc. of the 13<sup>th</sup> International Zeolite and Mesoporous Materials at the Dawn of the 21<sup>st</sup> Century*, eds. A., Galarneau, F., Di Renzo F., Fajula & Vedrine, Microporous and Mesoporous Materials: France, 0-P-15 Poster, 2001.
- [10] Zhao D., Zhou J. and Liu N., Preparation and characterization of Mingguang palygorskite supported with silver and copper for antibacterial behavior. *Applied Clay Science*, **33**, pp. 161–170, 2006.
- [11] Rivera-Garza M., Olguín M. T., García-Sosa I., Alcántara D., and Rodríguez- Fuentes G., Silver supported on natural Mexican zeolite as an antibacterial material, *Microporous and Mesoporous Materials*, **39**, pp. 431–444, 2000.
- [12] C. Ratiu, C. Lazau, P. Sfirloaga, C. Orha, D. Sonea, S. Novaconi, F. Manea and G. Burtica, I. Grozescu, Decontaminate effect of the functionalized materials with undoped and doped (Ag) TiO<sub>2</sub> nanocrystals, *Environmental Engineering and Management Journal*, **8(2)**, pp. 237, 2009.